arXiv:1510.03615v2 [cond-mat.mtrl-sci] 3 Feb 2016

Ab initio Investigation of Effect of Vacancy on Dissociation of Water Molecule on Cu(111) Surface

Vaibhav Kaware, [a,b†*] and Kavita Joshi [a‡*]

Water dissociation is a rate limiting step in many industrially important chemical reactions. In this investigation, climbing image nudged elastic band (CINEB) method, within the framework of density functional theory, is used to report the activation energies (E_a) of water dissociation on Cu(111) surface with a vacancy. Introduction of vacancy results in a reduced coordination of the dissociated products, which facilitates their availability for reactions that involve water dissociation as an intermediate step. Activation energy for dissociation of water reduces by nearly 0.2 eV on Cu(111) surface with vacancy, in comparison with that of pristine Cu(111) surface. We also find that surface modification of the Cu upper surface is one of the possible pathways to dissociate water when the vacancy is introduced. Activation energy, and the minimum energy path (MEP) leading to the transition state remain same for various product configurations. CINEB corresponding to hydrogen gas evolution is also performed which shows that it is a two step process involving water dissociation. We conclude that the introduction of vacancy facilitates the water dissociation reaction, by reducing the activation energy by about 20%.

1 Introduction

Water is of immense importance in many physio-chemical, biological, and chemical reactions.[1–8] It interacts with almost all solid surfaces that it comes in contact with, in one way or the other. It is ubiquitously present in naturally occurring phenomena and is important in industrial chemical reactions like methanol synthesis, steam reformation, and the water gas shift reaction (WGSR), to name a few.[1–5] It is also a strong candidate for production of hydrogen gas for the future technology of hydrogen fuel cells. Splitting water into hydrogen gas in contact with the electrode surfaces, holds the key to building more efficient and effective fuel cells.[9–13] Water dissociation reaction serves as a stereotypical example for model building of other complex reactions as well.[14] However, the simplicity of interaction of water with surfaces is only deceptive, since it is this interaction that leads to formation of water structures on metal surfaces that are far from being similar.[14] Since water is central to so many important chemical reactions, it is worth investigating its behaviour on various surfaces in search of better catalysts for its reactions. Interaction of water with Cu surface is of special importance for the WGSR. WGSR is a process in which the poisonous CO gas reacts with water, and gets converted into CO_2 and hydrogen gas. The reaction is typically used for production of hydrogen gas, and further into ammonia in industries like fertilizers and petroleum. Low temperature WGSR uses a mixture of oxides of Cu, Zn, Cr, Al, and others as catalyst, in varying proportions. However, active component of the catalyst at low temperature, is copper metal crystallite.[2] In spite of being well studied, there is no unanimously agreed mechanism for the working of WGSR. Interestingly, dissociation of water remains a crucial step in the WGSR, irrespective of the mechanism that drives it. Water dissociation becomes all the more important in WGSR and other reactions involving water dissociation, since it is the rate limiting step in all of them, along with other intermediate processes.[2,15] Thus, investigating water dissociation in varied environments and on different surfaces, becomes an essential task.

Dissociation of water has been studied on various pristine surfaces, computationally, as well as experimentally.[14,16–18] It dissociates on different pristine surfaces with varying degree of ease, wherein the activation energy for its dissociation varies from 0.15 eV on Si(110) to 1.36 eV on Cu(111).[15,19] It is observed that for almost all of these metal surfaces, water stabilizes parallel to the plane of surface atoms. The reason being that the highest occupied molecular orbital, $1b^1$, of water molecule is perpendicular to its plane. Orbital $1b^1$ interacts with the surface atoms, which orients it parallel to the slab surface.[18] Cu(111) is special as far as its interaction with water is concerned. Water is known to bind weakly to Cu(111).[18] It provides a good surface for dissociation reaction, since it lies at the delicate balance between wetting and de-wetting behavior with water. This means that the binding of de-wetting water on Cu(111) can be made either stronger, or can be further weakened by modifying the surface appropriately. As far as catalytic surfaces are concerned, it is also known that introduction of structural defects like kinks and steps activates the metal surface chemically for reactions like NO dissociation, O_2 dissociation, and CO oxidation, along with water dissociation.[20–23] Dissociation of water has been carried out previously on pristine Cu(111) surfaces, along with other pristine surfaces.[24–26] Fajín et. al. found that the presence of steps on Cu surfaces reduces the activation energy of water dissociation reaction.[27] They concluded that the low coordination along the steps is responsible for this behaviour. However, apart from steps and kinks, it is also possible to reduce the coordination on pristine surfaces by the creation of a vacancy defect.

In this work, we study water dissociation on Cu(111) surface in presence of a single atom vacancy. Vacancy on the surface of pristine Cu(111) surface gives rise to non-uniformity, unlike on pristine Cu(111), that provides the reactants with a variety in coordination to choose from. We have studied the changes in adsorption energies and geometries of the reactant and the products, the minimum energy path, and the activation energies in

[a]*Physical and Materials Chemistry Division, CSIR-National Chemical Laboratory, Pune, India - 411008*

[b]*Department of Physics, Savitribai Phule Pune University, Ganeshkhind, India - 411007*

‡*k.joshi@ncl.res.in,* †*v.kaware@ncl.res.in, vaibhav.kaware@gmail.com*

these cases. It is the aim of this study to verify the changes, if any, in activation energy of water dissociation on copper (111) surface, with vacancy. We also study the site dependence of reactant, and product molecules and the activation energy. The study is expected to emulate not only the defective copper surface as catalyst, but also copper nanoparticles that inevidently posses such defects, which may be used to catalyse the reaction.

2 Computational Details

Kohn-Sham formulation of density function theory (DFT) is used to calculate total energies and to optimize various structures. Projector Augmented Wave pseudopotential[28,29] is used, with Perdew Burke Ernzerhof (PBE)[30] approximation for the exchange - correlation and generalized gradient approximation,[31] as implemented in the plane wave code, Quantum Espresso (QE).[32] Van der Waals type interaction is incorporated in the calculation of energies.[33–35] Energy cutoff for plane-waves is kept at 47 Ry, and 221 Ry for charge density. Solid Bulk Cu was relaxed in a variable cell to obtain lattice parameter of 3.62 Å, which is in agreement with the reported experimental value of 3.62 Å.[36] A slab of 6 layers of atoms along the direction (111) and of 2x2 surface coverage, was then cut, and a single Cu atom vacancy was created. This slab was then relaxed, with all atoms free to move. Convergence of total energy with respect to varying cutoffs, k-points and vacuum along z-direction was confirmed. A monkhorst-pack grid of 4x4x1 k-points provided for a precision of better than 0.02 eV in the energy differences. A vacuum equivalent of 8 layers of unitcell, along (111) direction, (16.864 Å) was found to be sufficient to avoid image interaction in the z-direction. Forces were converged below 0.001 eV/Å during all optimizations, and below 0.1 eV/Å for all CINEB calculations. Nine intermediate images were used for all the CINEB calculations initially. Although CINEB calculations are known to be highly computation intensive, multiple such runs were performed with increased number of intermediate images, in order to span multiple pathways of the reaction in as much detail as possible, and to validate the initially found MEPs. The dissociation energy is defined as $E_{dissociation} = E_{IS} - E_{FS}$, while the adsorption energy is calculated as $E_{adsorption} = E_{suf+adsorbant} - (E_{surf} + E_{adsorbant})$. Here, E_{IS} is the total energy of the reactant, slab+H_2O, E_{FS} is the total energy of the product, viz., slab + 'dissociated water', $E_{slab+adsorbant}$ is the total energy of slab with the adsorbed water molecule, E_{slab} is the total energy of the standalone slab, and $E_{adsorbant}$ is the energy of adsorbed molecule in its free/gaseous state.

3 Results and Discussion

As discussed in the introduction, water dissociation is a rate limiting step in many industrially important chemical reactions, like water gas shift reaction. It is the aim of this work to study the effect of vacancy on the activation energy of water dissociation on Cu(111). CINEB calculations are used to calculate the activation energies, along with the MEPs.[37–39] Nudged elastic band method is a chain of states method, used to find the MEP between two local minima on the potential energy surface. Highest energy configuration along the MEP is the transition state (TS), which is used to calculate the reaction rate, within the harmonic transition state theory (hTST) approximation. Climbing image method is used to promote the transition state, found by NEB, to the saddle point.[39] Using CINEB calculations to find the MEP and the transition state requires that the two local minima, the initial (IS) and the final (FS) state, be known. In our case, the IS comprises of optimized slab+H_2O, while the FS is 'dissociated water'+slab. For the surface simulated here, there are more than one available choices to place H_2O molecule, and the product moieties. Hence, calculations in this work were initiated with multiple optimizations for the IS as well as FS. Eleven different non-equivalent positions were identified on the 2x2x6 slab, consisting of six vertex and 5 bridge positions. These positions are shown in Fig. 1. Vertex positions are positions in which the molecule was kept above the specific Cu atom site, and bridge position implied placing the desired molecule between two Cu atomic sites. Optimizations for initial (IS) and the final (FS) state were carried out on the fully relaxed Cu(111)+vacancy slab. The optimization of Cu(111)+vacany slab resulted in its expansion along (111) direction by about 1%. The vacancy site did not deform, expand or contract. All atoms were kept free to move during all optimizations on the slab, and also during the CINEB calculations.

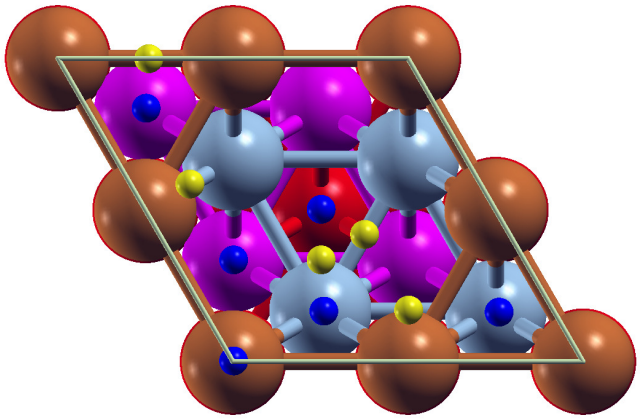

Fig. 1 (Color online) Non equivalent positions in a single cell. Vertex positions are colored blue, while bridge positions are colored yellow. Cu atoms in different planes are colored different in order to aid the eye. Brown colored spheres represent topmost layer 'A' of Cu atoms, while grey spheres signify the Cu atoms in layer 'B'. Magenta colored spheres are Cu atoms in layer 'C', and red spheres in layer D. The ABCABC stacking of Cu atom planes in pristine Cu along (111) direction, is introduced with stacking plane D which is same as stacking plane A, but with a vacancy. Hence, stacking order is DBCABC for the 6 layers considered in these calculations.

3.1 H_2O on Cu(111)+vacancy

For the initial state of reaction, water molecule was kept at predesignated distinct vertex sites (shown in Fig. 1), and the bridge sites, and their optimizations were carried out. It is reported that pristine Cu(111) aligns the H_2O molecule parallel to (111) direction.[15,24,26] Our calculations agree to the same, where water molecule aligns parallel to the (111) planes slightly off the atop position of Cu atom on pristine Cu(111) surface. Upon introduction of the vacancy, we found that irrespective of the

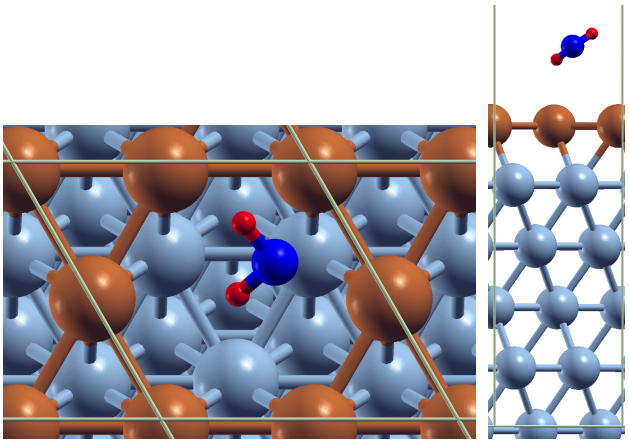

(a) (b)

Fig. 2 (Color online) The optimized position of water molecule on the slab (a) along (111) z-direction, (b) lateral view. Topmost layer of copper atoms is signified by brown spheres, whereas the Cu atoms in layers below, are all colored as gray spheres for the visual aid. Red colored spheres represent the H atoms, while blue colored spheres stand for O atom.

Surface	E_{ads} (eV)	h (Å)	d_{HO} (Å)	∠HOH (°)	tilt (°)	h_{ads} (Å)	O_{xy} (Å)
pristine Cu(111)	0.23	2.92	0.97	104	5.0	0.09	0.39
Cu(111)+vacancy	0.26	2.83	0.97	104	37.66	-	-

Table 1 Table of various distances and angles, with water adsorbed on respective slab. tilt: Tilting angle of plane of water molecule with respect to the Cu[111] plane. h:Distance between H_2O and slab. Value of E_{ads} compares well with adsorption energy values of 0.21 eV from Ref.[25], 0.18 eV from Ref.[15], and 0.24 eV from Ref.[18]. All other parameters compare well with those from Ref.[25].

initial position of water molecule, it always ended up lining at the vacancy site, with a slight inward tilt. With the vacancy in place, H_2O cannot stay entirely parallel to Cu(111) slab, and tilts downwards towards the slab. (Fig. 2). This is the degenerate global minimum energy configuration for water molecule to get adsorbed on the Cu(111)+vacancy slab. Slightly different angles and/or positions of water molecule at the vacancy result into degenerate energy configurations. H_2O stays adsorbed on the surface at ∼2.8 Å with adsorption energy of 0.26 eV. Comparison of the relevant parameters for water adsorbed on pristine and Cu(111)+vacancy, is produced in Table 1. Cases where the water molecule was kept at non-vacancy (pristine) site, the water molecule optimized into plane parallel to Cu(111) slab, as it would in case of the entire pristine Cu(111) slab. Adsorption energy of water molecule showed no change, whether the molecule ended up at the vacancy or at the pristine position. The reason behind this behaviour is that since water molecule is loosely adsorbed (via van der Waals interaction) on the Cu surface, changes in Cu surface may not strongly reflect in water adsorption.[18] However, modifying the surface may be expected to modify the behaviour of dissociated moieties, since they form chemical bonds with Cu atoms of the surface. Thus, in summary, water molecule on Cu(111)+vacancy slab optimizes in a degenerate position, where it tilts near the vacancy site. If placed upon high coordinated site, it prefers to stay planar, parallel to (111) direction, but its adsorption energy, does not change in either cases.

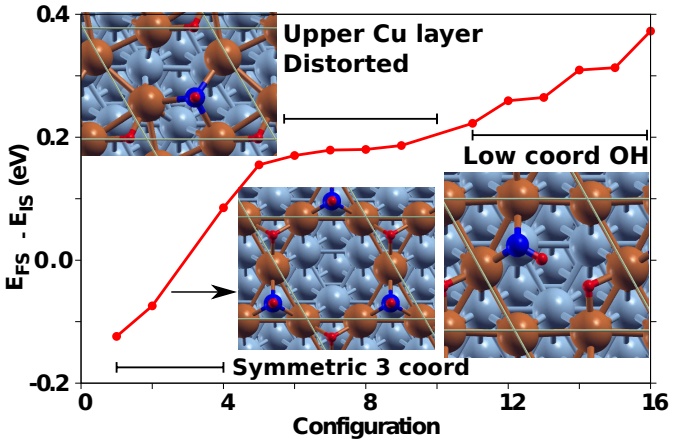

Fig. 3 (Color online) Various H+OH optimized configurations on Cu(111)+vacancy slab placed on the graph of their energies with respect to the IS energy. Coloring convention of spheres is same as in Fig. 2.

3.2 H+O+H on Cu(111)+vacancy

In order to arrive at conclusions about dissociated water, product atoms O, H, and H, were initially kept at different non-equivalent sites. Their optimizations led to the most common dissociation product of H+OH. Hence, OH was then placed at the vacancy site, and H atom was placed at various remaining positions, and optimized. In another set of optimizations, OH was kept at the vacancy site, at a distance of ∼2 Å above the slab, and different H atom positions were tried. A total of 27 combinations were optimized, which resulted into 16 distinct slab+products optimized geometries. These 16 distinct geometries were either distinct in positions, and/or in energies. Their dissociation energies spanned a range of about 0.6 eV. A concise representation of prominent of these geometries, along with their energies is shown in Fig. 3. These 16 configurations can be divided into three distinct classes based on their coordination with the surface. First, and the most prevalent type of configurations of FS are the ones in which H+OH are along the vacancy boundary (See Fig. 4(a)). In this configuration, both, H and OH, sit at the pristine Cu site, maximizing their coordination, with threefold equivalent bonds formed between H and three Cu atoms, and HO and three Cu atoms, respectively. This is the most stable FS configuration among all other FS configurations, and lies on the lower side of the graph in Fig. 3. In fact, the energy of this configuration is lower than the reactant, slab+H_2O, by ∼ 0.12 eV. The products avoid the vacancy in the most stable configuration, since their coordination cannot be increased at the vacancy site. The next class of FS consists of configurations in which H and OH maximize their coordination, by deforming the topmost layer of Cu atoms, within plane. This class consists of more than one kind of in-plane distortions of top Cu layers, in which the H and OH coordinate with either 2, or 3 Cu-atoms of the topmost

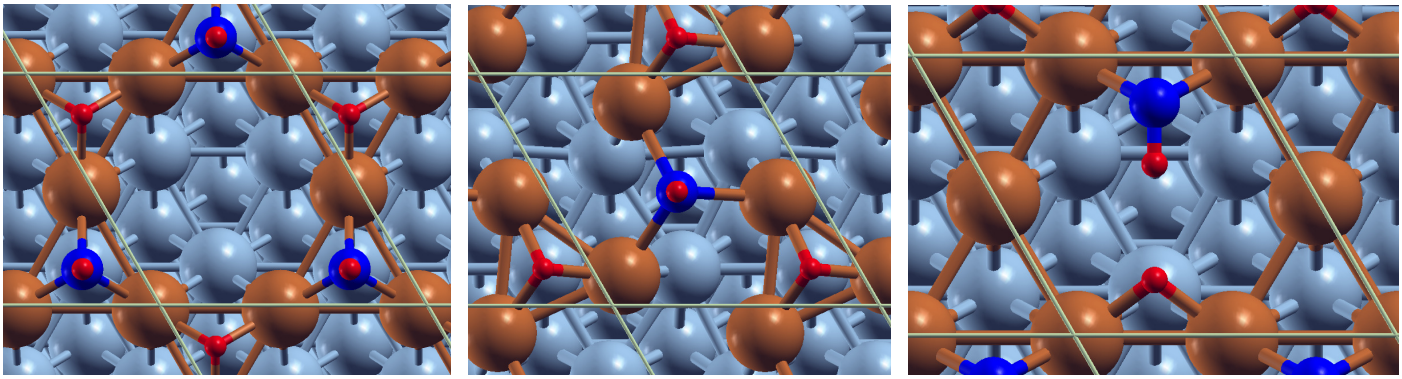

(a) (b) (c)

Fig. 4 (Color online) Representative configurations of H+OH+Cu(111)+vacancy for three types of FSs. Uppermost layer of Cu atoms is represented by brown colored spheres, while all Cu atoms in layers below are colored grey, for visual aid. H atoms are represented as red spheres, and O atoms as blue spheres. (a) The most prevalent, most stable configuration where H and OH bind at the pristine Cu site, around the vacancy. (b) Configuration in which H and OH coordination is maximized by distorting upper Cu-layer. (c) Low coordinated OH and H, with HO parallel to the Cu(111) plane.

plane. A representative configuration is shown in Fig. 4(b). The last class of optimized structures consists of HO being parallel to the Cu(111) plane, rather than being perpendicular to it, with lower (2-Cu) coordination. A distinct stable FS configuration was also reached upon optimization, that comprised of bound O atom, and adsorbed H_2 molecule. It is the only one, out of the 27 optimized configurations, which dissociates water in products other than H+OH.

Thus, symmetric arrangement of H+OH with 3 coordination is the most bound state of the products, while in least bound state, OH gets oriented parallel to (111) plane, with reduced coordination of 2.

3.3 NEB

Various optimizations for the initial and the final states of dissociation reaction give a single initial state for the reaction, and 16 different possible final states. NEB calculations are performed on 14 of these distinct final states. However, in some FS configurations, there were more than one possible ways in which water molecule split to give that particular FS configuration. Competing pathways of splitting H_2O, in such cases, did produce different activation energies during CINEB runs. We find that the activation energy for dissociation of water on Cu(111) slab with vacancy, is most commonly confined to range 1.04 – 1.18 eV. The FS in which H and OH are low-coordinated with two Cu atoms, possesses the least of activation energy (Top right part of Fig. 3), while the most stable of FS, in which H and OH form bonds with 3 Cu atoms along the periphery of vacancy, has the highest activation energy (See Fig. 4(a)).

Analysing the transition states (TSs) led us to the conclusion that there was a common trend in all these different MEPs. The activation energy in all the MEPs comprised of the step where water molecule on the slab gets closer to the slab, than their equilibrium distance, and attached itself to one of the Cu atoms. TS occurred in configuration in which actual splitting of this slab-bound water molecule takes place. Thus, the initial climb of the activation energy was found to be the same for all the MEPs. Since IS for all these CINEB calculations is identical, and also the MEP corresponding to activation energy climb, forward activation energies could be expected to be identical in all these calculations. Indeed, the forward activation energies varied only in a small range of 0.14 eV. Although the MEP of activation energy climb is similar for all the CINEBs, binding of water to the surface differs slightly with respect to the vacancy site, and the Cu atom positions. This is what introduces the variation of 0.14 eV in forward activation energy in spite of same IS and similar forward MEP.

Dissociation energies of the multiple FS configurations varied in the range of 0.6 eV. Since FS is not constant, unlike IS, variation in the FS's energies, and configurations, is reflected in an equally wide range in backward activation energy. Backward activation energy exhibits a marked trend with respect to (wrt) the energy of the FS. A graph of backward activation energies against the energy of the FS is shown in Fig. 5. Lower the energy of FS, harder it is to reform H_2O from the dissociated H+OH moieties. Hence, lower the energy of FS, greater will be the energy of activation to form H_2O from H+OH, and viceversa. Lowering of coordination of the dissociated H+OH products lowers their binding to the surface, also facilitating their easier removal from the surface for reactions that have water dissociation as an intermediate step. The classification of FS configurations, discussed earlier in section 3.2, also fits well with this variation. We see that all FSs in which H and OH bind with two Cu atoms, possess the least (backward) activation energy (0.33 – 0.78 eV). While, all FS in which the products H and OH are coordinated with 3 Cu atoms via distortion of the uppermost Cu surface, (0.82 – 1.02 eV) lie in between. The highest backward activation energies are exhibited by FS that possess the highest coordination, and high symmetry, bonding with 3 Cu atoms along the boundary of the vacancy (1.17–1.28 ev). Thus, low coordinated product states are conducive to lowering of the backward activation energy, while more symmetric arrangement of products corresponds to higher activation energy.

Further CINEB runs were performed for a few representative MEPs, with larger number of images (>20) in order to support

E_{FS} (eV)	E_a (eV)		Distance (Å)					
			HO-Cu			H-Cu		
	E_a^{Fwd}	E_a^{Bkwd}	1	2	3	1	2	3
Symmetric high coordinated FS								
-0.1238	1.15	1.28	2.04	2.04	2.04	1.73	1.74	1.74
-0.1238	1.06	1.19	2.04	2.04	2.04	1.73	1.74	1.74
-0.0742	1.09	1.17	2.05	2.05	2.05	1.73	1.73	1.73
Surface distorting FS								
0.1551	1.18	1.02	2.14	2.14	2.14	1.76	1.76	1.77
0.1791	1.09	0.91	2.14	2.15	2.16	1.71	1.79	1.82
0.1801	1.11	0.92	2.16	2.16	2.16	1.72	1.78	1.81
0.1865	1.11	0.92	2.16	2.17	2.17	1.74	1.76	1.78
0.2226	1.10	0.88	2.04	2.12	2.15	1.61	1.69	–
0.2593	1.08	0.82	2.00	2.00	–	1.64	1.64	–
Low coordinated products' FS								
0.3093	1.09	0.78	1.97	1.98	–	1.65	1.65	–
0.3131	1.06	0.74	2.01	2.01	–	1.64	1.64	–
0.3727	1.11	0.74	1.98	1.99	–	1.64	1.65	–

Table 2 Changes in bondlengths and activation energies (E_a) with decreasing binding between dissociated products and the Cu atoms of the Cu(111) slab + vacancy.

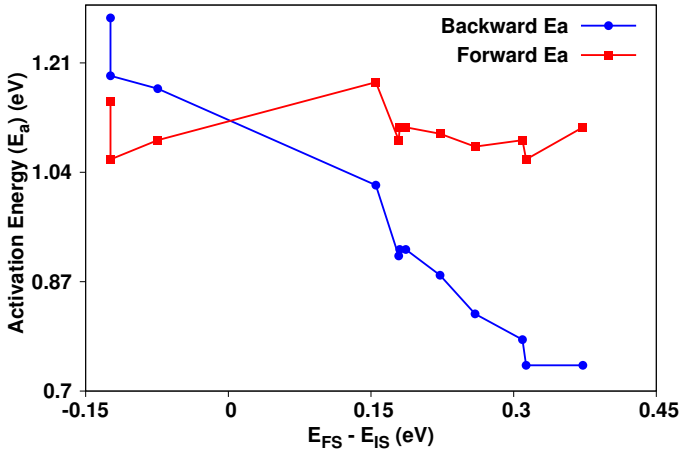

Fig. 5 (Color online) Forward and backward activation energy as a function of energy of FS configuration with respect to the IS energy. While forward activation energy (square points in red color) is almost constant for different FSs, a systematic decrease in backward activation energies (filled circles in blue color) is observed with increasing energy of FS. Higher the energy of the FS, lower is the binding of product moieties with the Cu(111)+vacancy slab.

our conclusions. MEP of FS geometry with symmetric 3 Cu coordinated OH and H was recalculated using varying number of images (25, 44 images, and partially fixed slab with 9 images). Activation energy of this configuration changed from 1.33 eV with 9 images, to 1.16 eV, when 25, as well as 44 images were used. Activation energy turned out to be 1.16 eV when 9 images were used with partially fixed slab (See Fig. 6). Along with the symmetric FS's NEB, a geometry in which OH and H exhibited low coordination (2) was also repeated with increased number of NEB images. It was chosen to represent the low coordination FS class. A CINEB with 50 images was performed as an extension to the already performed CINEB of 9 images. We found that its activation energy remained unchanged upon increasing the number of images from 9 to 50. Interestingly, the reaction in which H_2O dissociates into $O+H_2$, exhibited a drastic change in activation energy from 2.67 eV to 1.61 eV, when number of images was increased from 9 to 50. The 9-image MEP became a two step process when 50 images were used. The first step in the newly found MEP involved dissociation of H_2O into H+OH with energy of $\sim$ 1 eV, similar to other $H_2O \longrightarrow H + OH$ MEPs. The later part of the 50-image MEP involved breaking of OH bond while O remaining attached to the Cu atom, into H and O, so that finally $H_2 + O$ products are formed. Activation energy of the second part of MEP was 1.61 eV (See Fig. 7).

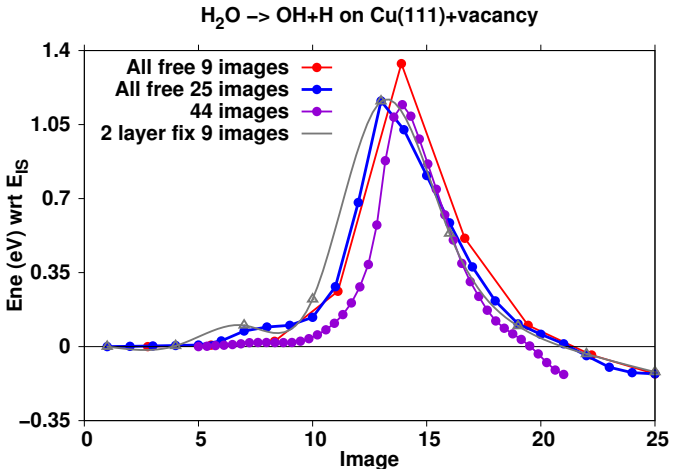

Fig. 6 (Color online) Increasing the intermediate images lowers E_a from 1.33 eV to 1.16 eV. Increasing intermediate images further did not changed the E_a from 1.16 eV .

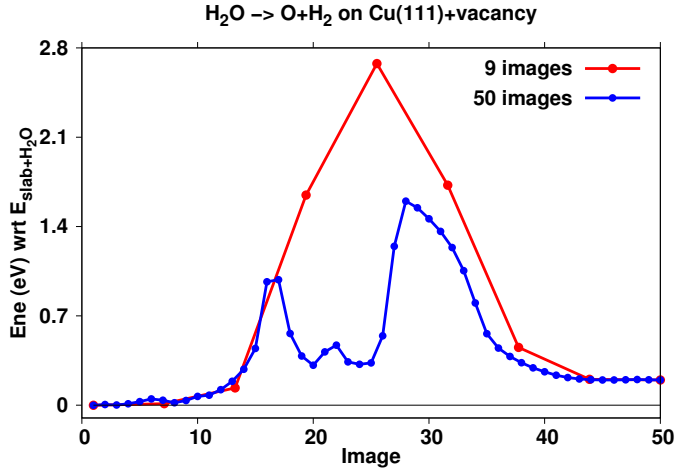

Fig. 7 (Color online) MEP of reaction in which water dissociated initially into $O+H_2$. Increasing the number of images shows that the reaction is a two step process. First step in which H_2O dissociates into H+OH (First peak 1.0 eV), and then OH further dissociates into O+H, (Second peak 1.61 eV), so that ultimately, O ends up bound to the surface, and free H_2 is formed in the final state.

4 conclusions

In this computational exercise we have demonstrated that introduction of vacancy defect in the Cu(111) pristine surface is one possible way to reduce the activation energy of water dissociation. Activation energy of water dissociation can be lowered by as much as 20% with introduction of a vacancy on the otherwise pristine Cu(111) surface. Weak interaction of water molecule with the copper surface is largely unaffected by the introduction of vacancy, which reflects in 'almost constant' forward activation energy that differs only slightly for different MEPs. The backward activation energies show a marked trend of decrease with lowering of coordination of the product moieties. We have also shown that breaking the symmetry of pristine surface by vacancy formation gives way to surface reconstruction, which opens up a new possibility to lower the activation energies of the reaction, that is otherwise absent in pristine surfaces. Activation energy of the route of 'surface reconstruction' is intermediate in terms of binding energy, and activation energy, between the low coordinated low binding product states, and high symmetry higher coordinated product states. We find that activation energy is a result of the adsorbed water molecule approaching the slab, closer than its equilibrium distance, and getting chemically bonded to the surface. Transition state is the configuration in which water splits at this attachment onto the slab. CINEB calculations carried out with large number of images showed that breaking of water into $O + H_2$ is a two step process that involves dissociation of water into $H + OH$ as an intermediate step.

In view of the above results, we feel that the effect of density of vacancy upon activation energy is a worthy investigation for future work.

5 Acknowledgements

The authors thank MSM (CSC-0129) for the financial support. CSIR-4PI and CDAC are gratefully acknowledged for availing their computational facility, used to carry out this work.

References

1 Ib Chorkendorff and Johannes W Niemantsverdriet. *Concepts of modern catalysis and kinetics*. John Wiley & Sons, 2006.

2 RJ Smith, Muruganandam Loganathan, Murthy Shekhar Shantha, et al. A review of the water gas shift reaction kinetics. *International Journal of Chemical Reactor Engineering*, 8(1), 2010.

3 CV Ovesen, BS Clausen, BS Hammershøi, G Steffensen, T Askgaard, Ib Chorkendorff, Jens Kehlet Nørskov, PB Rasmussen, Per Stoltze, and P Taylor. A microkinetic analysis of the water–gas shift reaction under industrial conditions. *Journal of Catalysis*, 158(1):170–180, 1996.

4 Alexander Ya Rozovskii and Galina I Lin. Fundamentals of methanol synthesis and decomposition. *Topics in Catalysis*, 22(3-4):137–150, 2003.

5 Sandra Sá, Hugo Silva, Lúcia Brandão, José M Sousa, and Adélio Mendes. Catalysts for methanol steam reforming–A review. *Applied Catalysis B: Environmental*, 99(1):43–57, 2010.

6 Philip Ball. Water as an active constituent in cell biology. *Chemical Reviews*, 108(1):74–108, 2008.

7 Biman Bagchi. *Water in Biological and Chemical Processes: From Structure and Dynamics to Function*. Cambridge University Press, 2013.

8 Philippa M Wiggins. Role of water in some biological processes. *Microbiological Reviews*, 54(4):432–449, 1990.

9 Artificial photosynthesis for solar water-splitting. *Naure Photonics*, 6:511–518, 2012.

10 M. S. Dresselhaus and I. L. Thomas. Alternative energy technologies. *Nature*, 414:332–337, 2001.

11 Michael G Walter, Emily L Warren, James R McKone, Shannon W Boettcher, Qixi Mi, Elizabeth A Santori, and Nathan S Lewis. Solar water splitting cells. *Chemical Reviews*, 110(11):6446–6473, 2010.

12 Frank E Osterloh. Inorganic nanostructures for photoelectrochemical and photocatalytic water splitting. *Chemical Society Reviews*, 42(6):2294–2320, 2013.

13 Michael Grätzeil. Photoelectrochemical cells. *Nature*, 414:338–344, 2001.

14 Javier Carrasco, Andrew Hodgson, and Angelos Michaelides. A molecular perspective of water at metal interfaces. *Nature Materials*, 11(8):667–674, 2012.

15 Amit A Gokhale, James A Dumesic, and Manos Mavrikakis. On the mechanism of low-temperature water gas shift reaction on copper. *Journal of the American Chemical Society*, 130(4):1402–1414, 2008.

16 Patricia A Thiel and Theodore E Madey. The interaction of water with solid surfaces: Fundamental aspects. *Surface Science Reports*, 7(6):211–385, 1987.

17 Michael A Henderson. The interaction of water with solid surfaces: fundamental aspects revisited. *Surface Science Reports*, 46(1):1–308, 2002.

18 A Hodgson and S Haq. Water adsorption and the wetting of metal surfaces. *Surface Science Reports*, 64(9):381–451, 2009.

19 Jun-Hyung Cho, Kwang S Kim, Sung-Hoon Lee, and Myung-Ho Kang. Dissociative adsorption of water on the Si(001) surface: A first-principles study. *Physical Review B*, 61(7):4503, 2000.

20 CP Vinod, JW Niemantsverdriet, and BE Nieuwenhuys. Interaction of small molecules with Au (310): Decomposition of NO. *Applied Catalysis A: General*, 291(1):93–97, 2005.

21 Ioannis N Remediakis, Nuria Lopez, and Jens K Nørskov. CO oxidation on gold nanoparticles: Theoretical studies. *Applied Catalysis A: General*, 291(1):13–20, 2005.

22 Michael A Henderson. Structural sensitivity in the dissociation of water on TiO_2 single-crystal surfaces. *Langmuir*, 12(21):5093–5098, 1996.

23 José LC Fajín, M Natália DS Cordeiro, and José RB Gomes. Adsorption of atomic and molecular oxygen on the Au(321) surface: DFT study. *The Journal of Physical Chemistry C*, 111(46):17311–17321, 2007.

24 A Michaelides, VA Ranea, PL De Andres, and DA King. General model for water monomer adsorption on close-packed

transition and noble metal surfaces. *Physical Review Letters*, 90(21):216102, 2003.

25 Abhijit A Phatak, W Nicholas Delgass, Fabio H Ribeiro, and William F Schneider. Density functional theory comparison of water dissociation steps on Cu, Au, Ni, Pd, and Pt. *The Journal of Physical Chemistry C*, 113(17):7269–7276, 2009.

26 Bin Jiang, Xuefeng Ren, Daiqian Xie, and Hua Guo. Enhancing dissociative chemisorption of H_2O on $Cu(_{111})$ via vibrational excitation. *Proceedings of the National Academy of Sciences*, 109(26):10224–10227, 2012.

27 José LC Fajín, M Natália DS Cordeiro, Francesc Illas, and José RB Gomes. Influence of step sites in the molecular mechanism of the water gas shift reaction catalyzed by copper. *Journal of Catalysis*, 268(1):131–141, 2009.

28 P. E. Blöchl. Projector augmented-wave method. *Physical Review B*, 50:17953–17979, Dec 1994.

29 G. Kresse and D. Joubert. From ultrasoft pseudopotentials to the projector augmented-wave method. *Physical Review B*, 59:1758–1775, Jan 1999.

30 John P. Perdew, Kieron Burke, and Matthias Ernzerhof. Generalized gradient approximation made simple. *Physical Review Letters*, 77:3865–3868, Oct 1996.

31 John P. Perdew, Kieron Burke, and Matthias Ernzerhof. Generalized gradient approximation made simple [Phys. Rev. Lett. 77, 3865 (1996)]. *Physical Review Letters*, 78:1396–1396, Feb 1997.

32 Paolo Giannozzi, Stefano Baroni, Nicola Bonini, Matteo Calandra, Roberto Car, Carlo Cavazzoni, Davide Ceresoli, Guido L Chiarotti, Matteo Cococcioni, Ismaila Dabo, et al. QUANTUM ESPRESSO: a modular and open-source software project for quantum simulations of materials. *Journal of Physics: Condensed Matter*, 21(39):395502, 2009.

33 M. Dion, H. Rydberg, E. Schröder, D. C. Langreth, and B. I. Lundqvist. Van der Waals density functional for general geometries. *Physical Review Letters*, 92:246401, Jun 2004.

34 T. Thonhauser, Valentino R. Cooper, Shen Li, Aaron Puzder, Per Hyldgaard, and David C. Langreth. Van der Waals density functional: Self-consistent potential and the nature of the van der Waals bond. *Physical Review B*, 92:125112, Sep 2007.

35 Guillermo Román-Pérez and José M. Soler. Efficient implementation of a van der Waals density functional: Application to double-wall carbon nanotubes. *Physical Review Letters*, 103:096102, Aug 2009.

36 Ralph Wyckoff. WG crystal structures. *New York, Interscience Publishers*, 1:7–83, 1963.

37 Daniel Sheppard, Rye Terrell, and Graeme Henkelman. Optimization methods for finding minimum energy paths. *The Journal of Chemical Physics*, 128(13):134106, 2008.

38 Graeme Henkelman and Hannes Jónsson. Improved tangent estimate in the nudged elastic band method for finding minimum energy paths and saddle points. *The Journal of Chemical Physics*, 113(22):9978–9985, 2000.

39 Graeme Henkelman, Blas P Uberuaga, and Hannes Jónsson. A climbing image nudged elastic band method for finding saddle points and minimum energy paths. *The Journal of Chemical Physics*, 113(22):9901–9904, 2000.